Journal of Nano- and Electronic Physics
Vol. **18** No 1, 01001(12pp) (2026)

Журнал нано- та електронної фізики
Том **18** № 1, 01001(12cc) (2026)

OPEN ACCESS

REVIEW

Design and Implementation of a Compact Wideband Wearable Antenna for ISM/WiMAX/WiFi/5G Band Body-Centric Wireless Applications

Md. Mehedi Hasan, Abu Zafor Md. Touhidul Islam* ✉

Antenna Design Lab, Department of Electrical and Electronic Engineering, University of Rajshahi, Rajshahi-6205, Bangladesh

(Received 22 July 2025; revised manuscript received 18 February 2026; published online 25 February 2026)

In this work, we propose a compact, wideband, and wearable microstrip patch antenna with a defected ground structure (DGS) for body-centric wireless applications. The proposed antenna, consists of an isosceles triangle with four parallel rectangular shaped flat bars, is designed and optimized in CST studio suite using low-cost FR-4 as the substrate with a height of 1.6 mm, relative permittivity of 4.3 and loss tangent of 0.025, followed by prototyping. The net geometry of the antenna is $35 \times 25 \times 1.6$ mm^3. A microstrip feed line is used to excite the antenna while rectangular slots on the antenna and partial grounding planes are used for improving the bandwidth. The designed antenna operates over a wide frequency range of 2.6 to 6.8 GHz which satisfy for the popular lower 5G, WiMAX, WiFi, and ISM band applications. The antenna resonates at of 3.5 GHz and 5.95 GHz, and maintains improved reflection coefficient, wide bandwidth, positive gain and efficiency over the operating frequency range. The on-body analysis of the simulation results available in CST has also been performed which shows reasonable results. The specific absorption rate (SAR) analysis is accomplished separately at each resonant peak frequency over a human body phantom model and the maximum SAR values obtained are 0.4137 W/kg at 3.5 GHz and 0.4062 W/kg 5.95 GHz for 1 gm of biological tissue which satisfy the IEEE recommended safety limit of 1.6 W/kg. A prototype of the proposed antenna is fabricated and the measured results of return loss shows good agreement with the simulated one. The combined features of new design, compact size, wideband performance, multiband support, improved reflection coefficient, positive gain and efficiency, and low SAR value contribute to the antenna's novelty, making the antenna a significant advancement in the field of wireless communication and biomedical applications.

Keywords: Wideband, Wearable, Triangular patch, 5G, WiMAX, WiFi, ISM Band, Phantom, SAR, WBAN.

DOI: 10.21272/jnep.18(1).01001 PACS number: 84.40.Ba

1. INTRODUCTION

Over the past decade, wearable antennas have gained significant popularity due to their diverse applications in health monitoring, diagnosis, tracking, and location sensing [1]. Their compact size, lightweight structure, affordability, and minimal maintenance make them highly desirable. These antennas are predominantly utilized in Wireless Body Area Networks (WBAN) systems, where they enable wireless connectivity between devices and the human body. Typically, wearable antennas are positioned at various locations on the body, working in unison to track biological signals such as glucose levels, blood pressure, and heart rate [2]. In body-to-body wireless communication, antennas worn by one individual interact with sensor nodes distributed across another person's body [3]. Despite their advantages, these antennas face certain limitations related to shape, size, substrate material properties, wearer comfort, robustness, structural deformation, and overall efficiency. Such constraints pose challenges for WBAN system designs operating in diverse radio frequency environments. Consequently, ongoing research focuses on developing robust and efficient antennas tailored for body-centric wireless communication [4].

The fifth generation (5G) network is already being used in several countries [5] and Internet of Things (IoT) use it to connect and exchange data among many interconnected wireless devices. Now wearable antennas become an indispensable part of IoT and are used in modern healthcare for monitoring patients' health diseases [6]. A set of frequency bands are designated to commercialize WBAN systems in the range 402 MHz to 10.6 GHz for the well-being of humanity [7, 8]. For designing an efficient and robust flexible antenna, it's essential for researcher to consider the possible design challenges in wearable applications [9] and to follow international safety rules defined for the human body [10]. In earlier studies [11-18], research has been done to design and analyze the performance of flexible wearable antennas with the aim of achieving design objectives. Different antenna structures comprising microstrip patch, planar monopole, Inverted-F planar, inkjet printed photopaper-based monopole, vertical monopoles, fractal, etc. have been studied. However, wideband and multiband antennas with low power consumption are becoming more wanted in the medical field [19]. The features of Microstrip antennas like small shape, light weight, low cost, low

* Correspondence e-mail: touhid.eee@ru.ac.bd

Cite this article as: Md. Mehedi Hasan et al., *J. Nano- Electron. Phys.* 18 No 1, 01001 (2026) https://doi.org/10.21272/jnep.18(1).01001

profile, ease of fabrication, and easy to integrate in a PCB, are crucial for wearable antenna design for 5G wireless communications and body-centric wireless medical systems [20]. The sub-6 GHz frequency spectrum (3.4 to 3.6 GHz) and 3.5 GHz center frequency have allowed in many countries for 5G communications [21, 22]. Researchers in [23, 24] have chosen low loss dielectric substrates like FR-4 to obtain required performance of the designed antenna. In [25, 26], wearable patch antennas have been designed on FR-4 substrate and designed antenna covers the popular WLAN, WiMAX, and C-bands. Their prototype antennas have overall dimensions of $60 \times 40 \times 0.254$ mm^3. A low-profile Meander line multiband antenna is proposed in [27] for WBAN application. In [28], a PDMS based wearable wideband antenna with the overall dimension is 24×38 mm is designed which operates from 3 to 6 GHz. A photopaper-based low-cost, wideband wearable antenna of overall size 30×40 mm^2 is proposed in [29] for WBAN applications which yielded 3 GHz bandwidth, 3.48 dBi gain and 84.35 %, radiation efficiency at the 5.2 GHz center frequency.

Although the reported microstrip antennas showed good performance results but suffer from some limitations like larger size, costly, narrow bandwidth, and so on. This manuscript presented a small size ($35 \times 25 \times 1.6$ mm^3) wideband (from 2.6 to 6.8 GHz) wearable antenna embedded with low-cost FR-4 substrate for WBAN applications. The designed antenna is applicable for the most popular lower 5G (3.33-4.2 GHz), WiMAX (3.4-3.6 GHz), WiFi-5 (5.15-5.85 GHz), and ISM (5.2-5.8 GHz) band applications. Simulation of the antenna has been done in CST Microwave Studio (MWS) software.

The paper is prepared as follows. Section 1 offers introduction to wideband flexible and wearable patch antennas, the related works, and research objectives. The proposed antenna structure and design details are presented in Section 2. Section 3 presents the simulated and measured results of the designed antenna under the off-body and on-body conditions, and SAR analysis. Section 4 provides performance comparison of the proposed antenna and the antennas designed in earlier studies. Finally, a conclusion is drawn in Section 5.

2. ANTENNA DESIGN METHODOLOGY

Initially, the proposed antenna's design, simulation, parametric investigation, numerical analysis of is carried out using the CST 2018 software under the off-body. The designed antenna is then fabricated and measured its properties in the laboratory via vector network analyzer. After that numerical study on the on-body analysis and SAR analysis of the designed antenna has been carried out using CST MWS software.

2.1 Geometry of the Proposed Antenna

The structure of the proposed antenna is illustrated in Fig. 1. It is designed and simulated by the Time Domain solver of CST MWS professional 3D EM software version 2018. Low loss FR-4 (Lossy) material, with a relative permittivity (ε_r) of 4.3 and a loss tangent (tan(δ)) of 0.025, is used as a substrate with a height of 1.6 mm. The antenna consists of an isosceles triangle with four parallel rectangular shaped flat bars. The antenna is exciting via the microstrip line feeding technique. The copper (annealed) of 0.035 mm thickness is used for construction of the ground plane, feedline, triangular patch with parallel bars. Initially, the antenna size (length and width) has been estimated using the set of basic equations, for 3.5 GHz resonance frequency. After that, the antenna design is optimized to a net size of $35 \times 25 \times 1.6$ mm^3, and two rectangular slots are added to the patch plane and partial ground plane to improve antenna's impedance matching and bandwidth. The first rectangular slot is used on the parallel bar 4 of the patch plane and the second rectangular slot is used on the partial ground plane to make defected ground structure.

The antenna's dimensions are optimized to a compact size of $35 \times 25 \times 1.6$ mm^3 with the use of parametric investigation. To make the size compact, we incorporated a patch plane consisting of an isosceles triangle with four parallel rectangular shaped flat bars. In order to decrease the effective electrical length of the antenna the reactive elements like parallel bars are used. Then slotted patch plane with partial ground and defected ground structures are used for the improvement of the antenna's performance. In the parametric investigation, we vary one design parameter at a time to observe its effect on the antenna's performance parameters (e.g., resonance frequency, reflection coefficient, gain, directivity, bandwidth, and efficiency). After completing optimization of one design parameter, we followed the same procedure to optimize the other parameters (e.g., the patch size, parallel bar length, feed point location, slot dimensions, partial ground dimensions, etc.).

Table 1 – Optimized design parameters of the proposed antenna

Design Parameter	Value (mm)
Width of ground (W_g)	25
Length of ground (L_g)	18
Ground slot dimension ($W_s \times L_s$)	4×8.3
Substrate width (W)	25
Substrate length (L)	35
Base length of triangle (Q)	22
Leg length of triangle (P)	13.04
Length of parallel bar (U/V/W/X)	20/17/13/8
Width of parallel flat bar (R/R/S/T)	1/1/1.5/4
Slot dimension on patch plane ($Y \times X$)	5.8×1.8
Width of feedline (W_f)	2.92
Length of feedline (L_f)	20

The length of the FR-4 substrate is chosen as 35 mm while the width as 25 mm. As seen from the front view of Fig. 1(a), the length of the base Q and leg P of the triangular part of the patch are 22 mm and 13.04 mm, respectively. The lengths (U, V, W, and X) and widths (R, R, S, and T) of four parallel rectangular shaped flat bars of the patch are defined in Table 1. To make sure 50 Ω impedance matching of the antenna, the feedline's length L_f of 20 mm and width W_f of 2.92 mm are chosen. Trial-and-error analysis is used for obtaining the rectangular slot dimensions ($Y \times Z = 5.8 \times 1.8$ mm^2) on the patch plane. The area of the partial ground plane is selected as 18×25

mm² and positioned at the lowermost side of the FR-4 substrate as shown in the back view of the antenna of Fig. 1(b). The dimension of ground slot is taken as ($W_s \times L_s = 4 \times 8.3$ mm²). Table 1 lists the optimized values of the design parameters of the proposed antenna.

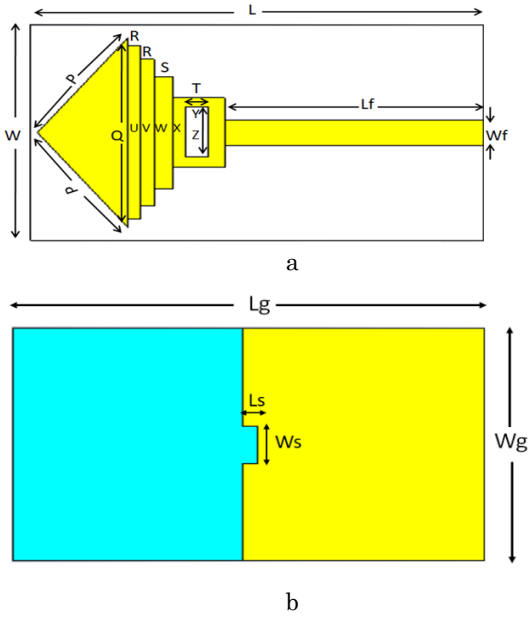

Fig. 1 – Geometric structure of the proposed antenna with (a) front view and (b) back view

2.2 Parametric Investigation

The effect of different geometrical parameters on resonant frequencies, bandwidth, and impedance matching properties of the antenna are analyzed in this section. The benefit of applying a rectangular slot on the patch plane is illustrated in Fig. 2(a). The plot shows that antenna with slot is providing reflection coefficient below -10dB in the frequency range 2.6 GHz to 6.8 GHz. The operating frequency range of the antenna exhibits two resonant frequencies at 3.5 and 5.95 GHz. The value of the reflection coefficient is about – 24.88 dB and – 16.38 dB at resonant frequency 3.5 GHz and 5.95 GHz. The use of slot reduces the reflection coefficient S11 and widen the bandwidth of the antenna.

The length and width of the feeder line is adjusted to obtain better impedance matching. The antenna shows lowest reflection coefficient for width of feeder line W_f = 2.92 mm (Fig. 2(b)) and length of feeder line L_f = 20 mm (Fig. 2(c)).

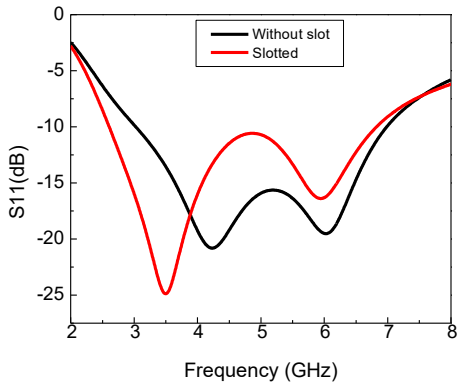

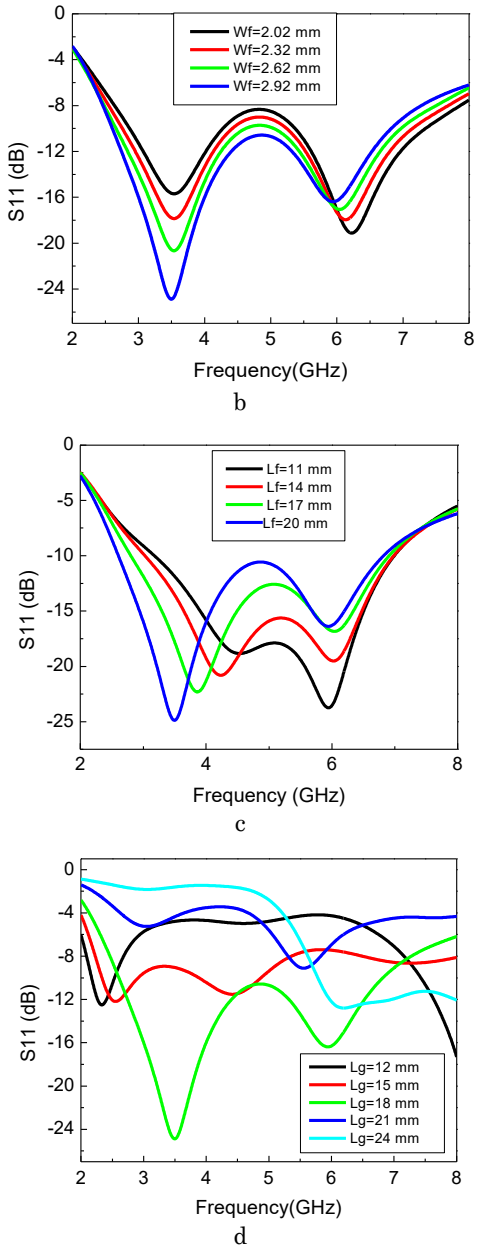

Fig. 2 – The effect of (a) slot (b) width of feeder line (c) length of feeder line (d) length of ground plane on the reflection coefficient (S11) of the proposed antenna

The use of partial ground in the designed antenna provides wide bandwidth and good impedance matching. The antenna shows minimum reflection coefficient for the length of partial ground L_g = 18 mm. The reflection coefficient is decreased with increasing L_g from 12 mm, attains lowest at 18 mm, then increased again with increasing Lg as shown in Fig. 2(d). With increasing W_g from 16 mm, the reflection coefficient is decreasing and the lower peak position shifting to higher frequency and reach 3.5 GHz at W_g = 25 mm as shown in Fig. 3(a). The advantage of using rectangular slot on the partial ground plane is illustrated in Fig. 3(b). The plot shows that antenna with partial ground slot provides reflection coefficient below – 10 dB in the wider range 2.6 to 6.8 GHz. By using rectangular slot of the ground plane, the operating frequency is adjusted to resonate at 3.5. As shown in Figs. 4(a) and (b),

the antenna exhibits high gain and efficiency over the complete working band from 2.6 to 6.8 GHz for L_g = 18 mm and W_g = 25 mm.

The minimum return loss and maximum gain, bandwidth and efficiency of the proposed antenna are obtained for the set of design parameters obtained from these parametric studies are presented in Table 1. Hence this set of parameters can be selected as the optimized parameters.

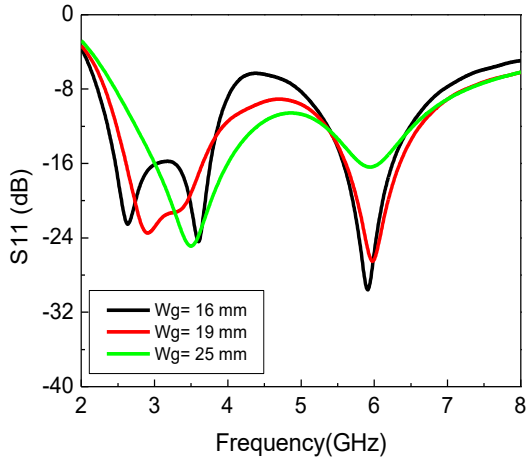

a

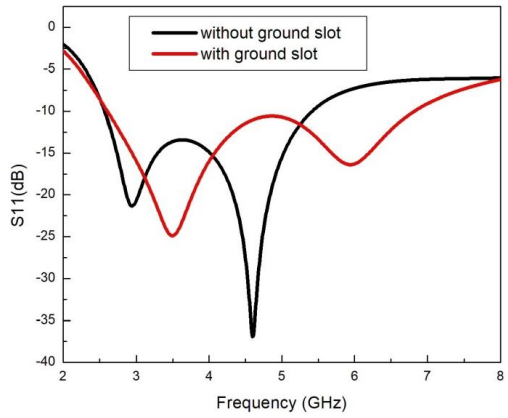

b

Fig. 3 – The effect of (a) width of ground plane (b) ground slot on the reflection coefficient (S11)

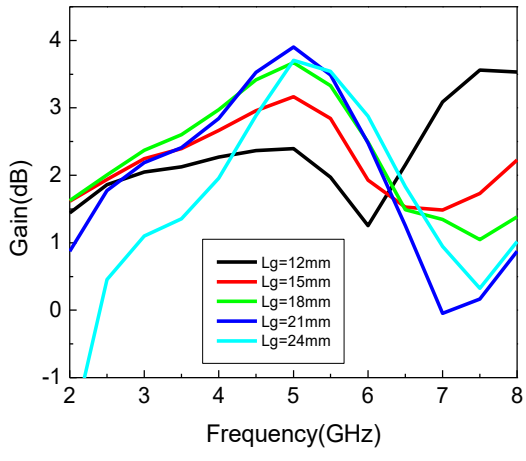

a

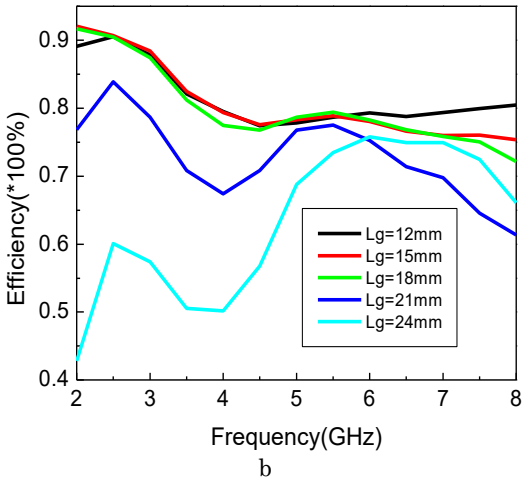

b

Fig. 4 – The effect of length of partial ground on the (a) gain (b) antenna efficiency

3. RESULTS AND DISCUSSION

3.1 Off-Body Numerical and Experimental Results

The proposed wearable patch antenna is fabricated and the front and back view of it is shown in Fig. 5. The reflection coefficient and voltage standing wave ratio of the developed antenna are measured in free space using LiteVNA 64. The experimental setup for the measurement is shown in Fig. 6. The measuring frequency range of this VNA is from 50 Hz to 6.3 GHz. Due to the absence of an anechoic chamber in the laboratory, radiation pattern, gain, and efficiency could not be measured.

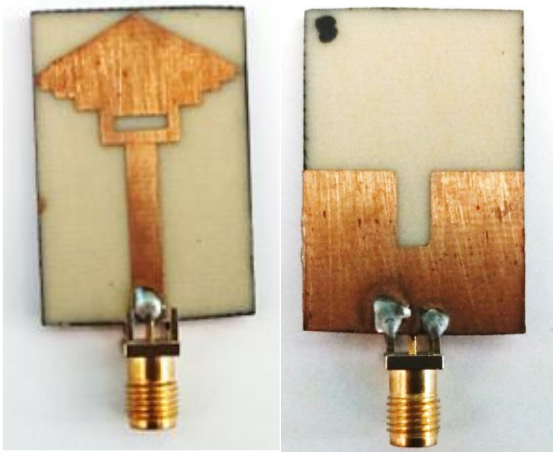

a b

Fig. 5 – (a) Front and (b) back view of the fabricated antenna

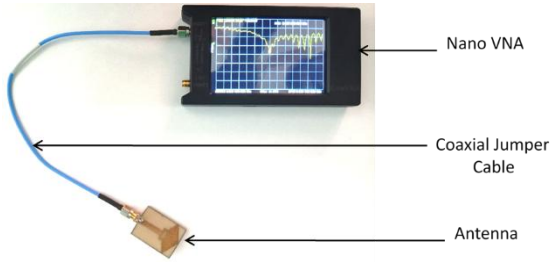

Fig. 6 – Setup for measurement

3.1.1 Reflection Coefficient

Figure 7 illustrates the variation of the reflection coefficient (S11) acquired by simulation and measurement versus frequency. The antenna exhibits two resonant frequencies around 3.5 and 5.95 GHz. The value of the return loss is about – 24.88 dB and 16.38 dB at resonant frequency of 3.5 GHz and 5.95 GHz, respectively. The operating -10 dB bandwidth of the proposed antenna is 4.2 GHz (from 2.6 to 6.8 GHz) covering the most popular lower 5G (3.33-4.2 GHz), WiMAX (3.4-3.6 GHz), WiFi (5.15-5.85 GHz) and ISM (5.2-5.8 GHz) band applications. Figure also shows the simulated resonant frequencies (3.5 GHz and 5.95 GHz) are close to measured resonant frequencies (3.65 GHz and 5.1 GHz) of the designed antenna. The values of the reflection coefficient at resonant peak frequencies are – 24.88 dB and – 16.38 dB (simulated) and – 35.18 dB and – 21 dB (measured). The value of the voltage standing wave ratio (VSWR) is obtained 1.12 (simulated) and 1.14 (measured), respectively. The experimental results deviated from the simulated results because of the presence of some manufacturing defects such as pure FR-4 was not used as substrate, etc.

Simulated Results of resonant frequencies are 3.5 GHz and 5.95 GHz, and the corresponding reflection coefficients are – 24.88 dB and – 16.38 dB. The measured results of resonant frequencies are 3.65 GHz and 5.1 GHz, and reflection coefficients are – 35.18 dB and – 21 dB, respectively. The measured resonant frequencies are slightly shifted compared to the simulated results, indicating minor discrepancies possibly due to fabrication tolerances, material imperfections, or measurement setup differences. The measured reflection coefficients are more negative, indicating better impedance matching in the experimental prototype compared to the simulation.

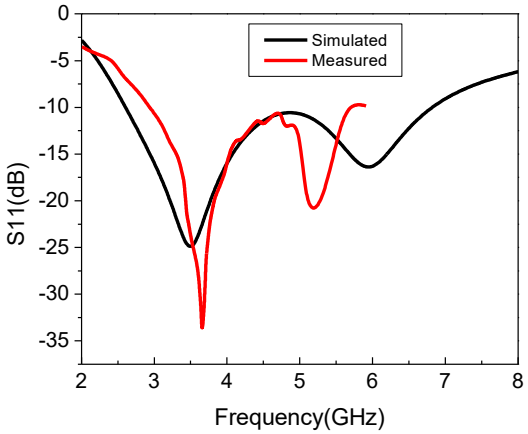

Fig. 7 – Reflection coefficient (S11) of the proposed antenna

3.1.2 Gain, Directivity and Efficiency

The 3D farfield gain and diectivity pattern of the proposed antenna at the resonant frequencies 3.50 GHz and 5.95 GHz are illustrated in Fig. 8 and 9, respectively. The maximum gain and directivity of the suggested antenna at 3,5 GHz are 2.6 dB and 3.51 dBi, while at 5.95 GHz, their corresponding values are 2.587 dB and 3.64 dBi. These figures also show valuable information about the performance characteristics of the antenna. The change of simulated gain and directivity against the operating frequency range is presented in Fig. 10(a).

Figure 10(b) shows the variation of antenna's radiation efficiency and total efficiency with frequency, displaying the radiation efficiencies are 81.17 % and 78.4 % at 3.5 GHz and 5.95 GHz, respectively. The antenna exhibits radiation efficiency in the range of 75.2 % to 91.4 % over the frequency range of operation. The proposed antenna is thus providing reasonable efficiencies at the resonating frequency in the operating range.

At 3.5 GHz, the antenna has a gain of 2.6 dB, VSWR of 1.12, and radiation efficiency of 81.17 %, and at 5.95 GHz, has a gain of 2.59 dB, VSWR of 1.35, and radiation efficiency of 78.4 %.

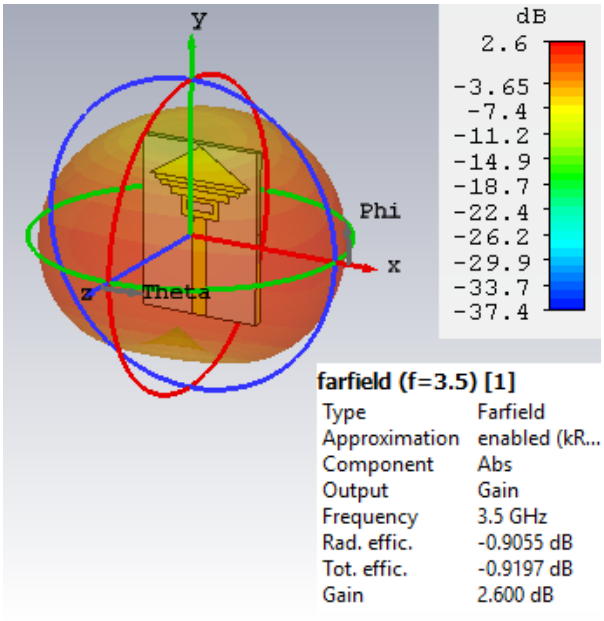

a

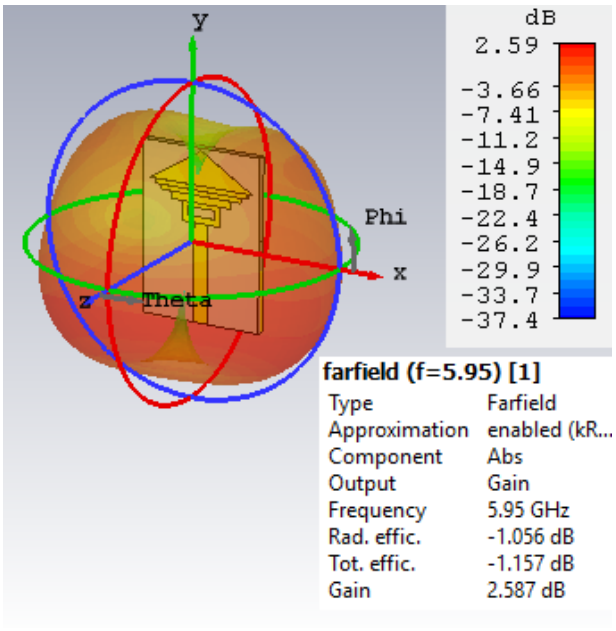

b

Fig. 8 – 3D farfield gain of the proposed antenna at (a) 3.5 GHz and (b) 5.95 GHz

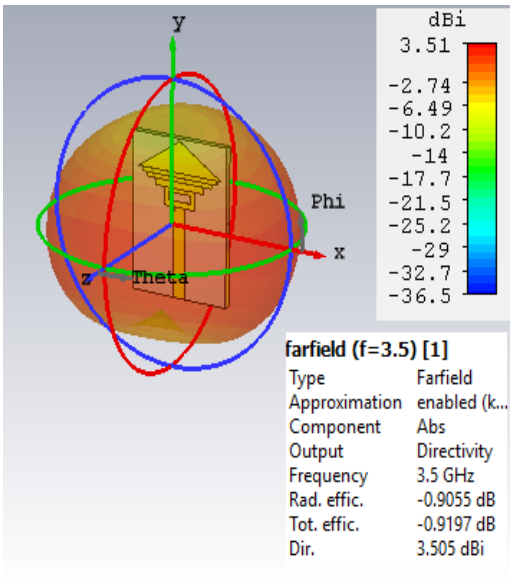

a

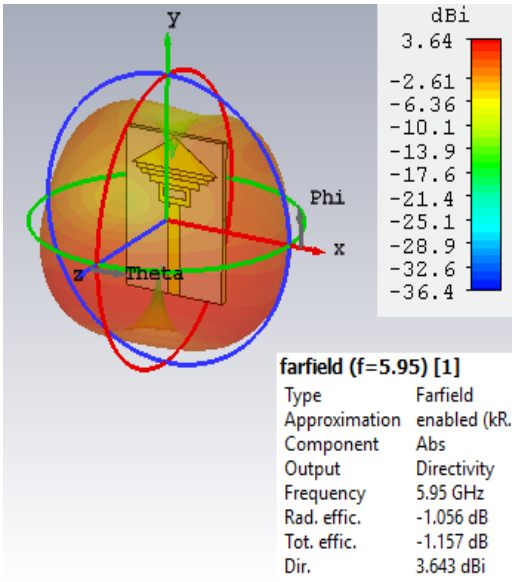

b

Fig. 9 – 3D farfield Directivity of the proposed antenna at (a) 3.5 GHz and (b) 5.95 GHz

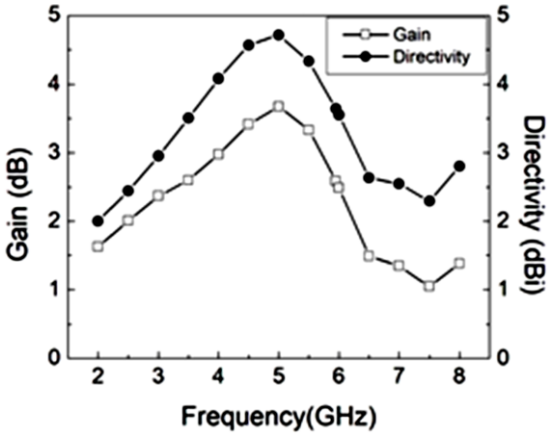

a

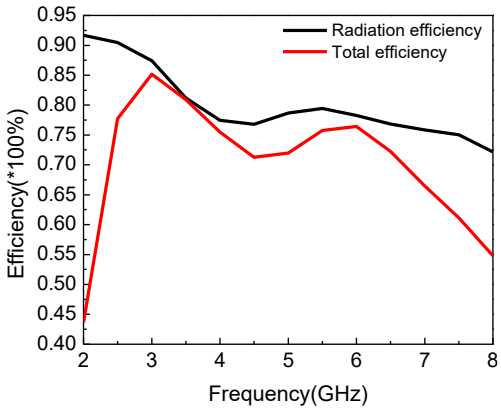

b

Fig. 10 – (a) Gain and directivity (b) Efficiency over operating frequency range

3.1.3 Radiation Pattern

Figure 11 illustrates the radiation pattern of the proposed antenna under the free space off-body condition. The main lobe magnitudes are 17.4- and 17.3-dB V/m at 3.5 and 5.95 GHz resonant peak frequencies, respectively. The corresponding main lobe directions are 163 and 144 degrees, the 3 dB angular beam-widths are 88.6 and 66.8 degrees, and the side lobe levels are – 2.4 and – 1.1 dB. The directional radiation pattern of the antenna making it suitable for popular applications in the lower 5G, WiMAX, WiFi, and ISM bands.

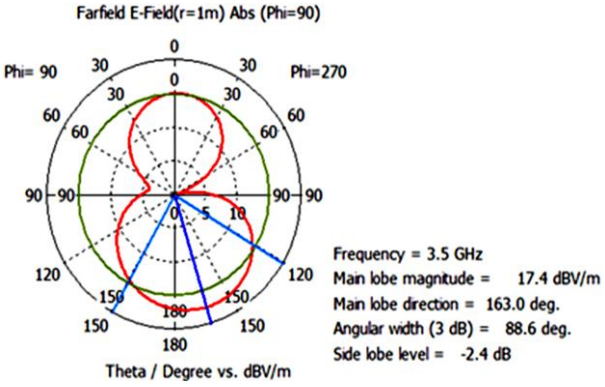

a

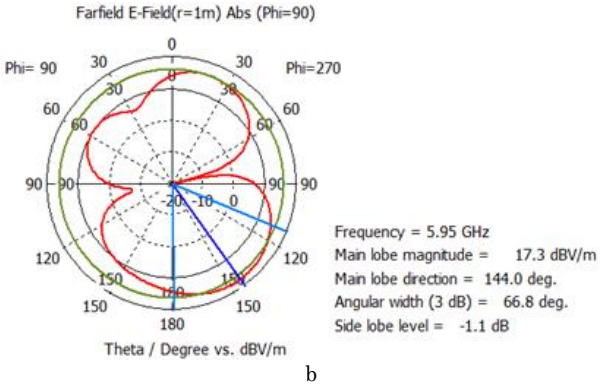

b

Fig. 11 – Farfield *E*-field pattern of the antenna at phi = 90° at (a) 3.5 GHz and (b) 5.95 GHz

3.1.4 Current Distribution

The current distribution at the surface of the designed antenna at the two resonant frequencies are shown in Figure 12 which presents the real electric current brought by the applied EM field throughout the antenna. As observed from the figure that the surface current originates from the microstrip line feed and mostly distributed at the lesser portion of the feed line and the inferior edges of the patch at both resonance frequencies. The maximum surface current density is 52.7395 A/m at 3.50 GHz and 52.1798 A/m at 5.95 GHz, and is as depicted in Figure 12 (a) and (b). The deployment of rectangular shaped flat parallel bars in the patch plane results in relatively higher current density at the bottom region of the patch and improves the radiation characteristics.

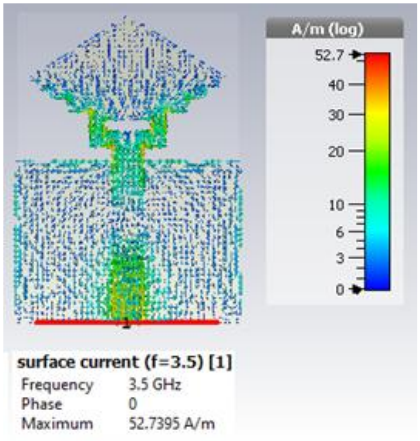

a

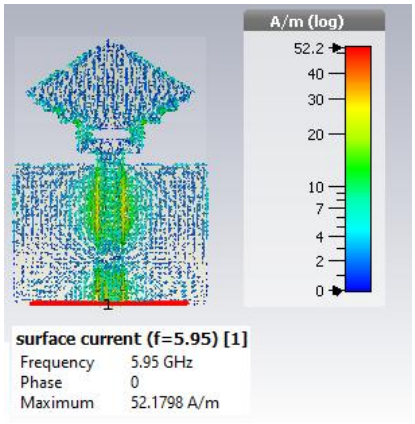

b

Fig. 12 – Proposed antenna's surface current distribution at (a) 3.5 GHz (b) 5.95 GHz

3.2 Antenna's On-Body Performance Analysis

The antenna's performance is analyzed under the off-body (free space) condition first and after that in on-body (on phantom) condition to observe the effect of the EM properties of human body tissues on the antenna performance parameters at higher frequencies. Moreover, different antenna parameters and SAR are also analyzed for varying separation between antenna and phantom and minimal separation for improved performance of the antenna has been determined.

3.2.1 Structure of 3D Phantom Model

To design antenna for WBAN applications, it is essential to analyze the antenna's performance within the three layers of the human body environment. So, a human body tissue equivalent phantom model is constructed using CST software by incorporating tissue properties as outlined in Table 2. Fig. 13 (a) illustrates the structure of a human body phantom model of size 25 mm × 35 mm × 36 mm using the three-layers of skin, fat and muscle tissues of thickness 1 mm, 10 mm and 25 mm, respectively. The properties of the three layers as depicted in Table 2 are estimated over the frequency range of 2.6 to 6.8 GHz using published reports [29, 30], and are used for the simulation of SAR at both the resonant frequencies of 3.5 and 5.95 GHz.

Table 2 – Estimated properties of skin, fat and muscle tissue layers

Tissue	Frequency (GHz)	Permittivity (ϵ_r)	Loss tangent	Conductivity σ (s/m)	Mass density (kg/m³)
Skin (dry)	3.5	37.005	0.28103	2.0249	1109
	5.95	34.988	0.3322	3.8473	
Fat	3.5	5.1739	0.15439	0.15553	911
	5.95	4.9412	0.18522	0.30294	
Muscle	3.5	51.444	0.25533	2.5575	1090
	5.95	48.284	0.32169	5.1414	

For obtaining optimum distance between the designed antenna and the body phantom, the reflection coefficient parameter is determined for both resonant frequencies of 3.5 and 5.95 GHz at six distinct separations and the estimated S11 values are showed in Table 3. It is seen that with the placement of antenna very close to the human body, the S11 values goes above – 10 dB and the resonance frequencies are detected to be shifted. Hence, 8 mm distance of between the antenna and skin is accepted as an optimum separation and the proposed antenna's convenient placement is determined to be over a suit or jacket instead of in direct contact with the human body.

Table 3 – Simulated reflection coefficient (S11) at different distances between antenna and skin

Distance (mm)	S11 (dB) at 3.5 GHz	S11 (dB) at 5.95 GHz
2	– 9.59	– 9.76
4	– 10.12	– 11.74
6	– 10.65	– 15.64
7	– 10.99	– 17.42
8	– 11.37	– 18.7
10	– 12.27	– 19.78

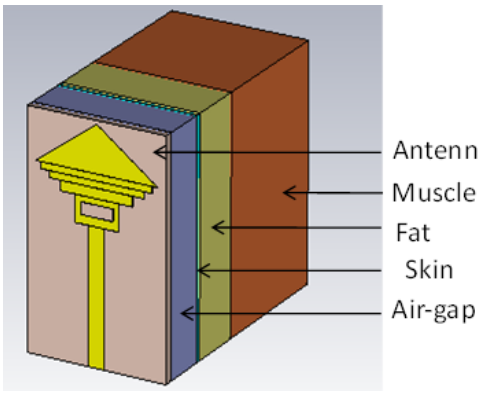

a

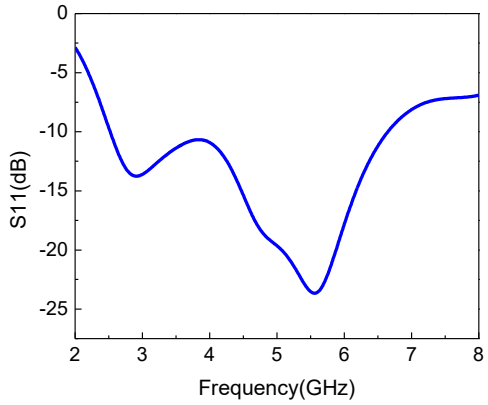

b

Fig. 13 – On-body performance of the antenna (a) 3D body phantom model, (b) S11 parameter

3.2.2 On-Body Simulated Results Analysis

3.2.2.1 Reflection Coefficient (S11 Parameter)

The proposed antenna's reflection coefficient (S11) on body phantom is shown in Fig. 13(b). The resonant peak frequency seemed to be slightly shifted to lower frequencies and the S11 values at 3.5 GHz and 5.95 GHz are – 11.37dB and – 18.7dB, respectively. At each resonant frequency, the S11 value is appeared well below -10 dB but noticed to be higher than the off-body condition value. It is also evident that the proposed antenna exabits a satisfactory wide bandwidth under the on-body conditions. The higher reflection coefficient may result from reactive loading by the body and variation of antenna's input impedance because of the fringing effect. Once the antenna is placed close to the human body, fringing effect may change the antenna's effective width and shifts the resonant frequency [27].

3.2.2.2 VSWR

The VSWR of the proposed antenna on body phantom is depicted in Fig. 14. The VSWR at 3.5 GHz and 5.95 GHz are 1.73 and 1.26, respectively. The results indicate sufficient impedance matching.

3.2.2.3 Gain, Directivity and Efficiency

Under the on-body condition, the designed antenna's gain, directivity and efficiency are analyzed at 3.5 GHz and 5.95 GHz resonant frequencies. The change of antenna's gain with frequency is depicted in Fig. 15 (a). Almost identical antenna's gain is observed at 5.95 GHz. However, as seen the gain is reduced in magnitude at 3.5 GHz as a result of EM energy absorption in the body tissue layers.

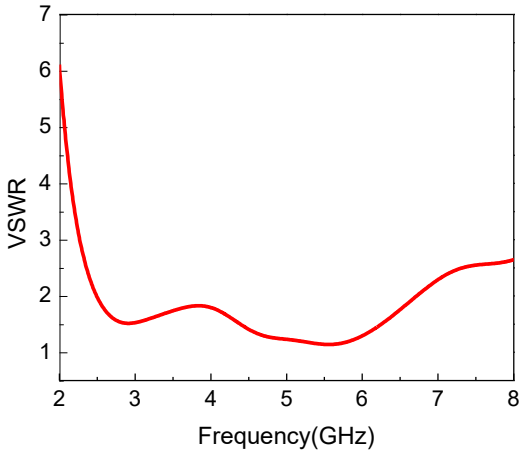

Fig. 14 – On-body simulated and measured VSWR of the proposed antenna

The 3D directivity patterns of the antenna on human body phantom model are depicted in Fig. 15 (b) for 3.5 Gz and in Fig. 15(c) for 5.95 GHz. The gain and directivity magnitudes of the proposed antenna are mentioned in Table 4, which demonstrate the antenna possesses sufficient amount of directivity for wireless transmission. The variation of radiation and total efficiencies of the designed antenna with frequency on human body phantom is depicted in Fig. 15(d), and the values at the resonant frequencies are summarized in Table 4. A significant reduction in efficiency is observed because of EM energy absorption in the tissue layers.

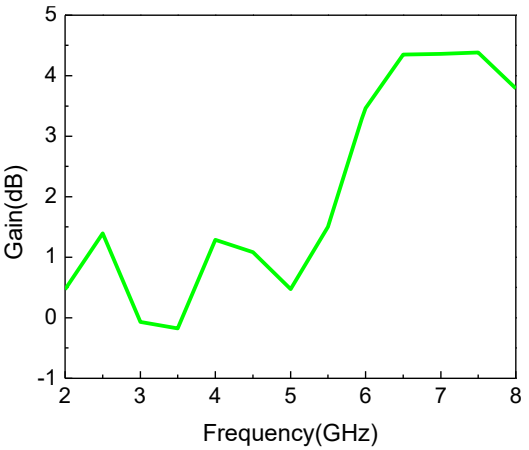

a

For 3.5 GHz, when the antenna is placed in on-body condition, the gain drops significantly from 2.6 dB to – 0.177 dB, indicating that the antenna's ability to direct power in a specific direction is compromised when placed on the body. Radiation efficiency decreases substantially from 81.17 % to 38.5 %, suggesting that more power is lost due to absorption and detuning effects caused by the body's

proximity. For 5.95 GHz, when the antenna is placed in on-body condition, the gain increases from 2.59 dB to 3.29 dB, which may result from favorable interactions between the antenna and the body's electromagnetic properties at this frequency. Radiation efficiency decreases from 78.4 % to 52.9 %, showing a moderate reduction in efficiency due to power absorption by the body.

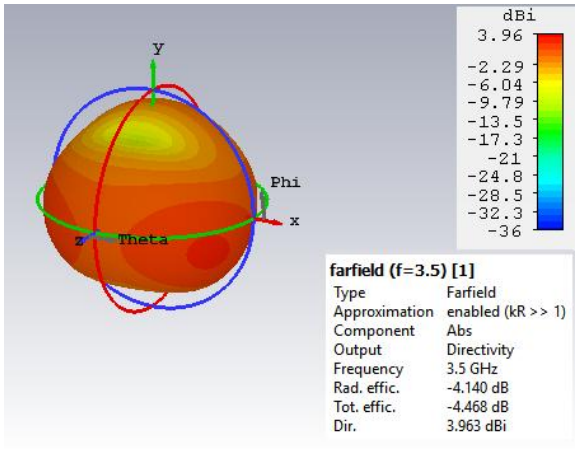

b

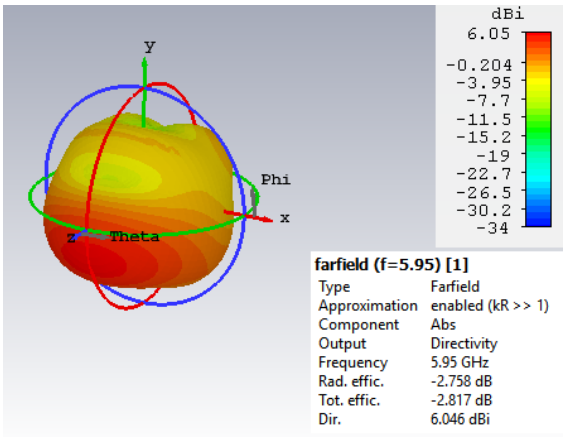

c

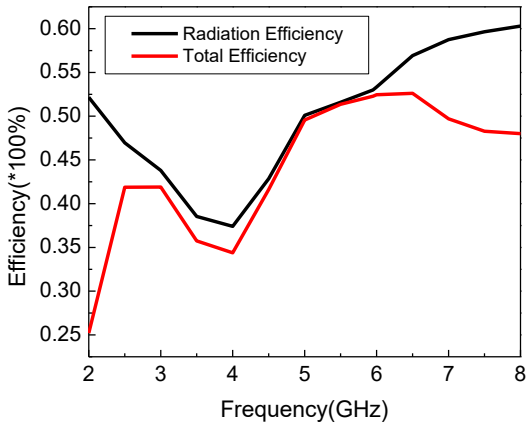

d

Fig. 15 – Simulated antenna's on-body (a) Gain, (b) Directivity at 3.5 GHz, (b) Directivity at 5.95 GHz and (c) Efficiency

Table 4 – Proposed antenna's on-body Gain, Directivity, and Radiation Efficiency

Resonance frequency (GHz)	Gain (dB)	Directivity (dBi)	Efficiency (%)
3.5	– 0.177	3.96	38.5
5.95	3.29	6.05	52.9

3.2.2.4 Radiation Pattern

At the resonant frequencies of 3.5 and 5.95 GHz, the antenna's radiation patterns over the human body phantom is shown in Fig. 16. As seen the radiation pattern is nearly directional which makes it suitable for the required most popular lower 5G, WiMAX, WiFi and ISM band applications. Fig. 16 depict the *E*-field of the far-field radiation pattern of the designed antenna over the human body phantom at 3.5 and 5.95 GHz at phi = 90 degrees.

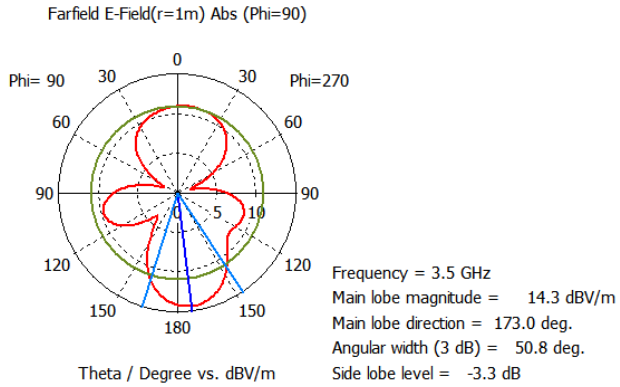

a

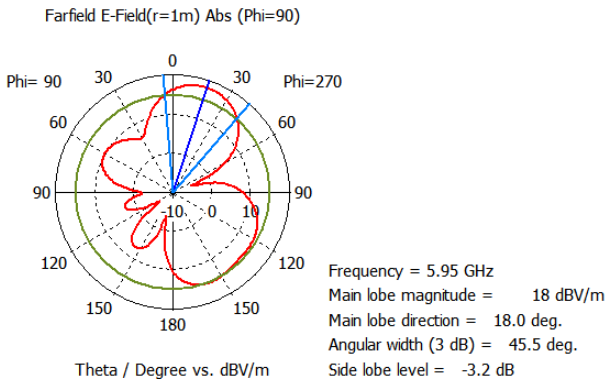

b

Fig. 16 – Antenna's radiation pattern on body phantom at (a) 3.5 GHz and (b) 5.95 GHz

At 3.5 GHz, the observed main lobe magnitude, the main lobe direction, angular width (3 dB) and side lobe level are 14.3 dBV/m, 173 degree, 50.8 degree and – 3.3 dB, respectively. While at 5.95 GHz, their corresponding values as observed to be 18 dBV/m, 18 degree, 45.5 degree and – 3.2 dB, respectively.

3.2.2.5 SAR Analysis of the Designed Antenna

The antenna's Specific Absorption Rate (SAR) is analyzed for 3.5 GHz and 5.95 GHz resonant frequency

under the placement of antenna on human body phantom model. The optimum separation of 8 mm between the antenna and skin has been chosen and the simulations are conducted under an input power of 5 mW. The SAR value is averaged over 1 g of biological tissue for the designed three-layer tissue phantom model. The US Federal Communications Commission (FCC) agency specified the standard safe limit of SAR value is 1.6 W/kg for 1 g of tissue. The simulation results of SAR distributions of the proposed antenna at 3.5 GHz and 5.95 GHz are shown in Figs. 17(a) and (b), respectively for 1 gm of tissue. The observed corresponding maximum SAR values are 0.4137 W/kg and 0.4062 W/kg, which are far below the standard threshold of safety limits defined by the FCC.

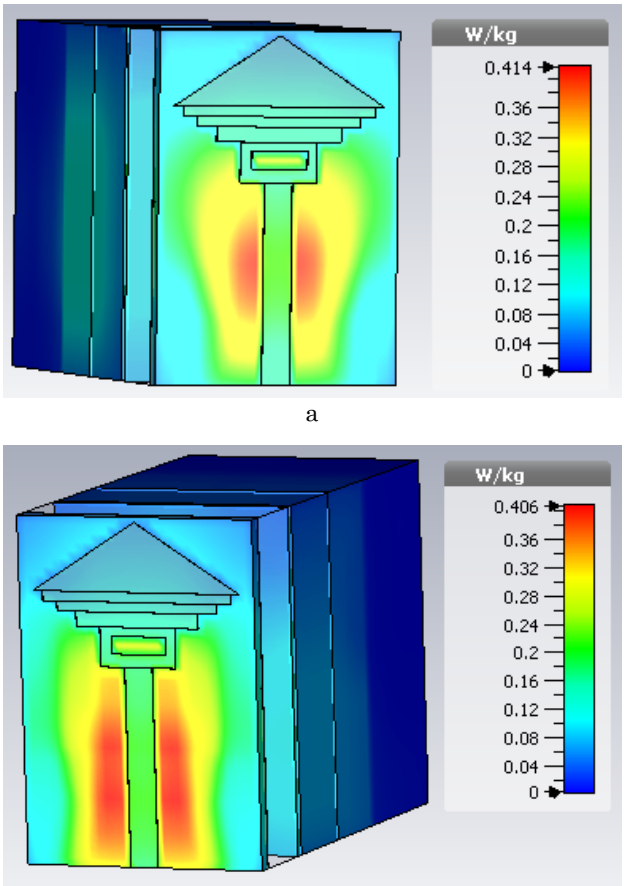

Fig. 17 – SAR analysis of the proposed antenna at (a) 3.5 GHz, (b) 5.95 GHz

4. COMPARISON OF PROPOSED ANTENNA WITH EXISTING RESEARCHES

The proposed antenna's performance has been compared with existing antennas performance as tabulated in Table 5. It is obvious from the table that our antenna is more compact, provides wider bandwidth, and reasonable gain. The SAR value of proposed antenna is observed to be lower than most of the reported antenna found in the literature and are far below the standard threshold of safety limits defined by the FCC.

The explanation of novelty of the work in terms of comparison with prior arts is as follows. Considering the size of the antenna, in earlier studies, wearable antennas for dual-resonance typically required larger areas to maintain efficient performance. In the proposed design, the isosceles triangular patch antenna with four parallel bars achieves dual-resonance functionality in a highly compact size of 35 × 25 × 1.6 mm^3. The reduced dimensions enhance usability and comfort for wearable applications. Seeing the bandwidth, most wearable antennas found in the literature achieved limited bandwidth (in some cases less than 2 GHz) due to their design constraints limiting their effectiveness for applications requiring broader frequency ranges. The proposed designed antenna achieved a wider bandwidth of 4.2 GHz (including the two resonant frequencies at 3.5 GHz and 5.95 GHz). This enhanced bandwidth supports diverse communication standards (e.g., 5G, WLAN) while maintaining stable performance in wearable environments. In view of SAR, many wearable designed antennas in prior arts face challenges in meeting safety standards due to high SAR values caused by their proximity to the human body. The proposed design used of FR-4 substrate and the optimized geometry of the antenna minimizes SAR while maintaining radiation efficiency. Many prior wearable antennas achieve dual-band operation but often operate in distinct frequency bands, leading to size and efficiency trade-offs. The proposed antenna resonates at 3.5 GHz and 5.95 GHz within a single broad bandwidth that is rare, allowing the design to cover multiple applications seamlessly.

Table 5 – Comparison of presented antenna with some of the existing researches

Ref. No.	Substrate Material/ε_r	Center Frequency (GHz)	Size (L×W×h) mm^3	Operating Frequency/ Bandwidth	SAR (W/Kg)	Gain (dBi)
[24]	Rogers RT 5880/2.2	3.47	35×31×0.79	2.87–5.47GHz/2.6 GHz	NR	2.647 dB
[8]	Photopaper/3.2	2.45, 3.5, 5.2	40 × 30 × 0.27	(2.30–5.30 GHz)/3 GHz	1.53(1g) & 1.93 (10g)	3.48
[31]	PDMS-gNWs/2.8	2.4	50×50×5.5	2.4-2.6 GHz	0.18 (1g)	2.4
[32]	FR-4/4.3	2.4	62 ×43× 1.67	2.3369-2.443 GHz/104 MHz	0.44 (1g)	0.86
[33]	Rogers TMM4	4.515, 5.065, 5.8487	36 × 30 × 1.524	NR	1.52, 1.3, 1.45 (1g)	3.6.96, 2.3
[34]	Felt	3.5	70×70×2	2.36-2.40 and 3.4-3.6 GHz	0.772	3.5
[35]	FR4/4.4	2.4	30×40×1.6 4	69.04%	0.98	3
[36]	FR4/4.4	1.7 and 2.45	81×54×1.6	1.57–2.39 and 2.38–2.58 GHz	NR	2.2 and 3.34 dB
This work	FR-4/4.3	3.5, 5.95	35×25×1.6	2.6 to 6.8 GHz / 4.2 GHz	0.4137 (1g) @ 3.5 GHz & 0.4206 (1g) @ 5.95 GHz	2.6

Abbreviation: NR for Not Reported

Targeted Applications of the proposed antenna is Healthcare Monitoring Systems for Continuous monitoring of vital signs such as heart rate, blood pressure, glucose levels, and body temperature. Following the monitoring, wireless data transmission between sensors and a central monitoring device. The proposed antenna is suitable for WBAN Applications due to the following reason. (i) Frequency Band Compatibility: 3.5 GHz falls in the Citizens Broadband Radio Service (CBRS) band, widely used for healthcare.5.95 GHz is part of the ISM band which is also suitable for WBAN applications. (ii) Low SAR Values: Maximum SAR values (0.4137 W/kg at

3.5 GHz and 0.4062 W/kg at 5.95 GHz) comply with IEEE standards (≤ 1.6 W/kg for 1 g of tissue), ensuring user safety. (iii) Compact Design: The isosceles triangular structure and FR-4 substrate result in a compact, lightweight design ideal for integration into wearable devices. (iv) Directional Radiation Pattern: Ensures efficient communication while minimizing interference with other body-mounted sensors.

5. CONCLUSION

In this paper, a novel wideband compact wearable microstrip patch antenna is designed and simulated using CST software for body-centric wireless applications to cover the most popular lower 5G, WiMAX, WiFi and ISM frequency bands. The antenna structure is developed on FR-4 substrate and consists of an isosceles triangle with four parallel rectangular shaped flat bars. A microstrip feed line is used to excite the antenna while rectangular slots on the antenna and partial grounding planes are used for improving the bandwidth and impedance matching, providing a net size of $35 \times 25 \times 1.6$ mm^3. The proposed antenna resonates at two frequencies of 3.5 GHz and 5.95 GHz and operates over a wide range from 2.6 to 6.8 GHz with a huge bandwidth of 4.2 GHz. The antenna is resonated at 3.5 GHz with a gain, VSWR, and radiation efficiency of 2.6 dB, 1.12, and 81.17 %, respectively and also at 5.95 GHz with the corresponding values of 2.59 dB, 1.35, and 78.4 %, respectively under the off-body condition. Under the on-body condition, the antenna offers reasonable values of performance parameters. Moreover, the antenna satisfies safety requirements with low SAR values of less than 1.6 W/kg for
1 gm of tissue. The proposed antenna's experimental prototype was fabricated and the measured results of reflection coefficient shows good agreement with the simulated one. The combined features of new design, compact size, wideband performance, multiband support, improved return ross, positive gain and efficiency, and low SAR value contribute to the antenna's novelty, making the antenna a suitable candidate for wireless communication and body-centric biomedical applications. values of less than 1.6 W/kg for 1 gm of tissue. The proposed antenna's experimental prototype was fabricated and the measured results of reflection coefficient shows good agreement with the simulated one. The combined features of new design, compact size, wideband performance, multiband support, improved return ross, positive gain and efficiency, and low SAR value contribute to the antenna's novelty, making the antenna a suitable candidate for wireless communication and body-centric biomedical applications.

AKNOWLEDGEMENTS

The authors would like to express gratitude to university for providing the resources and support necessary for this research. Authors also grateful for the guidance and encouragement from colleagues who have contributed valuable insights during the development of this work. Their support has been invaluable in completing this study.

REFERENCES

1. K.N. Paracha, S.K. Abdul Rahim, P.J. So, et al., *IEEE Access* **7**, 56694 (2019).
2. Z.H. Jiang, M.D. Gregory, D.H. Werner, *IEEE Trans. Biomed. Circ. Syst.* **10** No 2, 328 (2016).
3. T. Björninen, F. Yang, *IEEE Antennas Wireless Propag. Lett.* **15**, 794 (2016).
4. L. Fourati, *Proceedings of the 2014 IEEE International Conference on healthcare Informatics*, 362 (Verona, Italy: 2014).
5. K.V. Karad, V.S. Hendre, *Recent Treands in Electronics and Communication, Lecture Notes in Elcectrical Engineering* **777** (Sringer, Singapore: 2020).
6. S.M. Ali, C. Sovuthy, M.A. Imran, et al., *Micromachines* **11** No 10, 888 (2020).
7. J.F. Zhao, X.M. Chen, B.D. Liang, et al., *Wireless Commun. Mobile Comput.* 2017, 5842310 (2017).
8. A. Jabbar, M. Zubair, M.A. Naveed, et al., *IET Microwaves Antennas Propag.* **16** No 15, 962 (2022).
9. N.H.M. Rais, P.J. Soh, F. Malek, et al., *2009 Loughborough Antennas & Propagation Conference*, 225 (Loughborough, UK: 2009).
10. H.M. Madjar, *2016 International Symposium on Electromagnetic Compatibility-EMC EUROPE* (IEEE: Washington, USA: 2016).
11. M. Suma, P. Bybi, P. Mohanan, *Microw. Opt. Technol. Lett.* **48** No 5, 871 (2006).
12. A. Arif, M. Zubair, M. Ali, et al., *IEEE Antennas Wireless Propag. Lett.* **18** No 5, 981 (2019).
13. P.J. Soh, G.A.E. Vandenbosch, S.L. Ooi, N.H.M. Rais, *IEEE Trans. Antennas Propag.* **60** No 1, 379 (2012).
14. Y. Nechayev, P. Hall, Z. Hu, *IET Microw. Antennas Propag.* **4** No 6, 722 (2010).
15. S. Kim, Y.-J. Ren, H. Lee, et al., *IEEE Antennas Wireless Propag. Lett.* **11**, 663 (2012).
16. Akram Alomainy, Yang Hao, Abdus Owadally, et al., *IEEE Trans. Antennas Propag.* **55** No 1, 245 (2007).
17. H. Li, S. Sun, B. Wang, F. Wu, *IEEE Trans. Antennas Propag.* **66** No 6, 3136 (2018).
18. Sangeetha Velan, Esther Florence Sundarsingh, Malathi Kanagasabai, et al., *IEEE Antennas Wireless Propag. Lett.* **14**, 249 (2015).
19. A.T. Mobashsher, A.M. Abbosh, *IEEE Antennas Wireless Propag. Lett.* **15**, 1618 (2016).
20. S. Akinola, U. Hashimu, G. Singh, *International Conference on Computational Intelligence and Knowledge Economy (ICCIKE)*, 148 (2019).
21. N. Ferdous, G.C. Hock, S.H.A. Hamid, et al., *IOP Conf. Ser.: Earth Environ. Sci.* **268** No 1, 012152 (2019).
22. A. Boutejdar, B.I. Halim, S.E. Hani, et al., *International Journal of Electronics and Communication Engineering* **12**, 406 (2018).
23. L.C. Paul, M.U. Rashid, M. Mowla, et al., *IET 3rd International Conference on Electrical, Electronics, Engineering Trends, Communication, Optimization and Sciences (EEECOS)* (Tadepalligudem: 1-2 June 2016).
24. L.C. Paul, Md. T.R. Jim, T. Rani, et al., *Heliyon* **8**, No 10, e10934 (2022).
25. A. Dey, D. Mitra, W. Arif, *Proceedings of the 2021 IEEE International IoT, Electronics and Mechatronics Conference* (Toroto, Canada: 2021).
26. A. Dey, D. Mitra, W. Arif, *Int. J. RF Microw. Comput. Aided Eng.* **30**, e22459 (2020).
27. Tania Islam, Sayan Roy, *Electronics* **12**, 1416 (2023).
28. Wan Haszerila, Wan Hassan, Nga Yan Li, et al., *J. Phys. Conf. Ser.* **1502**, 012008 (2000).

29. P.A. Hasgall, F. Di Gennaro, C. Baumgartner, et al., *IT'IS Database for Thermal and Electromagnetic Parameters of Biological Tissues*, Version 4.1 (2022).
30. D. Andreuccetti, R. Fossi, C. Petrucci, *An Internet Resource for the Calculation of the Dielectric Properties of Body Tissues in the Frequency Range 10 Hz-100 GHz* (1997).
31. Zhi Hao Jiang, Zheng Cui, Taiwei Yue, et al., *IEEE Trans. Biomed. Circ. Syst.* **11** No 4, 920 (2017).
32. Shahid M. Ali, Varun Jeoti, Tale Saeidi, et al., *Indonesian Journal of Electrical Engineering and Computer Science* **15** No 3, 1509 (2019).
33. Tania Islam, Sayan Roy, *Electronics* **12**, 1416 (2023).
34. H. Yang, X. Liu, *IEEE Antennas Wireless Propag. Lett.* **19** No 12, 2324 (2020).
35. Shankar Bhattacharjee, Monojit Mitra, Sekhar R. Bhadra Chaudhuri, *Prog. Electromagn. Res. M* **55**, 143 (2017).
36. Vandana Yadav, Ram Suchit Yadav, Prakhar Yadav, et al., *AEU – Int. J. Electron. Commun.* **162**, 154576 (2023).

Розробка та виготовлення компактної широкосмугової антени для бездротових та застосувань в діапазонах ISM/WiMAX/WiFi/5G

Md. Mehedi Hasan, Abu Zafor Md. Touhidul Islam

Antenna Design Lab, Department of Electrical and Electronic Engineering, University of Rajshahi, Rajshahi-6205, Bangladesh

У цій роботі ми пропонуємо компактну, широкосмугову та носиму мікросмужкову патч-антену з дефектною заземлювальною структурою (DGS) для об'ємно-центрованих бездротових застосувань. Запропонована антена складається з рівнобедреного трикутника з чотирма паралельними прямокутними плоскими стрижнями, розроблена та оптимізована в студійному пакеті CST з використанням недорогого FR-4 як підкладки висотою 1,6 мм, відносною діелектричною проникністю 4,3 та тангенсом кута втрат 0,025, з подальшим створенням прототипу. Геометрія антени становить 35 × 25 × 1,6 мм3. Для збудження антени використовується мікросмужкова лінія живлення, а прямокутні пази на антені та часткові заземлювальні площини використовуються для покращення пропускної здатності. Розроблена антена працює в широкому діапазоні частот від 2,6 до 6,8 ГГц, що задовольняє популярні застосування в нижньому діапазоні 5G, WiMAX, WiFi та ISM. Антена резонує на частотах 3,5 ГГц та 5,95 ГГц і підтримує покращений коефіцієнт відбиття, широку смугу пропускання, позитивний коефіцієнт посилення та ефективність у всьому робочому діапазоні частот. Також було проведено аналіз результатів моделювання, доступних у CST, на тілі антени, який показує прийнятні результати. Аналіз питомого коефіцієнта поглинання (SAR) проводиться окремо на кожній резонансній піковій частоті на фантомній моделі людського тіла, і максимальні отримані значення SAR становлять 0,4137 Вт/кг при 3,5 ГГц та 0,4062 Вт/кг при 5,95 ГГц для 1 г біологічної тканини, що відповідає рекомендованому IEEE граничному значенню безпеки 1,6 Вт/кг. Виготовлено прототип запропонованої антени, і виміряні результати втрат на відбиття добре узгоджуються з результатами моделювання. Поєднання особливостей нової конструкції, компактних розмірів, широкосмугової продуктивності, підтримки кількох діапазонів, покращеного коефіцієнта відбиття, позитивного коефіцієнта посилення та ефективності, а також низького значення SAR сприяють новизні антени, роблячи її значним прогресом у галузі бездротового зв'язку та біомедичних застосувань.

Ключові слова: Широкосмуговий, Носимий, Трикутний патч, 5G, WiMAX, WiFi, ISM-діапазон, Фантомний, SAR, WBAN.